*photonics*

MDPI

# Supplementary Information

**Shiming Gan [1], Tianci Zhao [1], Xiuzhuang Mei [1], Tingting Zhang [1], Zhiqi Wang [1], Hongyu Gao [1], Gensen Yang [2], Jixiang Cai [1]*and Fuzhong Bai [1]***

[1] School of Mechanical Engineering, Inner Mongolia University of Technology, Hohhot 010051, China
[2] State Key Laboratory of Dynamic Measurement Technology, North University of China, Taiyuan 030051, China
* Correspondence: jxcai@imut.edu.cn; fzbaiim@163.com

## S1. Simulation methodology

Numerical simulations of structures are performed using the finite element method in a commercial software package CST Microwave Studio. The unit-cell boundary conditions are used along the *x*- and *y*-directions. For the *z*-direction, the open boundary conditions are employed [16, 36]. The refractive indexes of $TiO_2$ and Au are from the Palik's Handbook [35]. The theoretical results of the bifocal metalens are obtained by vectorial angular spectrum theory in Ref [44] (the Matlab code could be discovered in Ref [43]), and the simulated results are calculated by the finite integration method in the CST. The open boundary conditions are used along the *x*-, *y*-, and *z*-direction. The LCP/RCP light normally illuminates structures along the *z*-direction.

## S2. The positions of LS and ALS structures

Due to the designed LS structure without mirror symmetry, when the LS structure is symmetrized along its *y*-axis (black dashed line in Figure S1), the ALS structure is obtained with different origin coordinates. Therefore, when switching the incidence from LCP to RCP, the reflectance spectra of LS and ALS structures show some differences. Thus, the cut plane depicts slicing two arms of the LS structure in Figure 2(a)-(b) (in manuscript), but it cuts a single arm of the ALS structure in Figure 2(c)-(d).

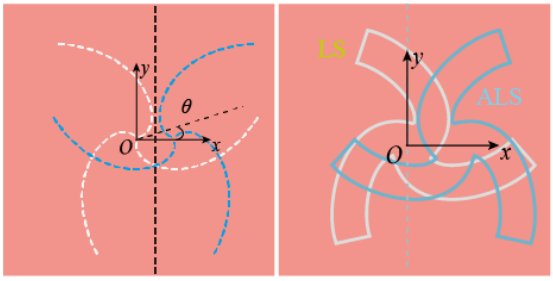



Figure S1 Schematic of positions of LS and ALS elements (center lines (left), and contour lines (right)).

## S3. Phase shifts in the broadband wavelength range

In the wavelength range of 560-660 nm, the phase shifts for the LC structure could cover the 0-2π range (when the orientation angles $\theta$ change 60° (in Figure S2)), which are agree well with theoretical expectations in Equation (1) in the manuscript.

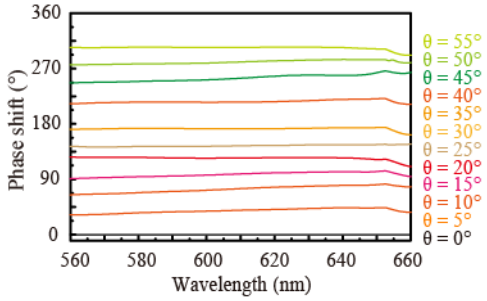



Figure S2 The simulated phase shifts at 560-660 nm.

## S4. The contour images of the two structures

The contour images of instantaneous electric and magnetic field distributions of unit cells are shown in Figure S3. The electric intensity of two LS structures for LCP incidence is stronger than that of RCP, but the magnetic intensity is approximately unchanged for LCP and RCP incidence as shown in Figure S3(b) (the influence of the magnetic field on the performance is small). However, the phenomenon is reversed for the ALS element in Figure S3(d). It also demonstrates that the different responses of the LS and ALS structures are mainly induced by electric field interaction for two spin states.

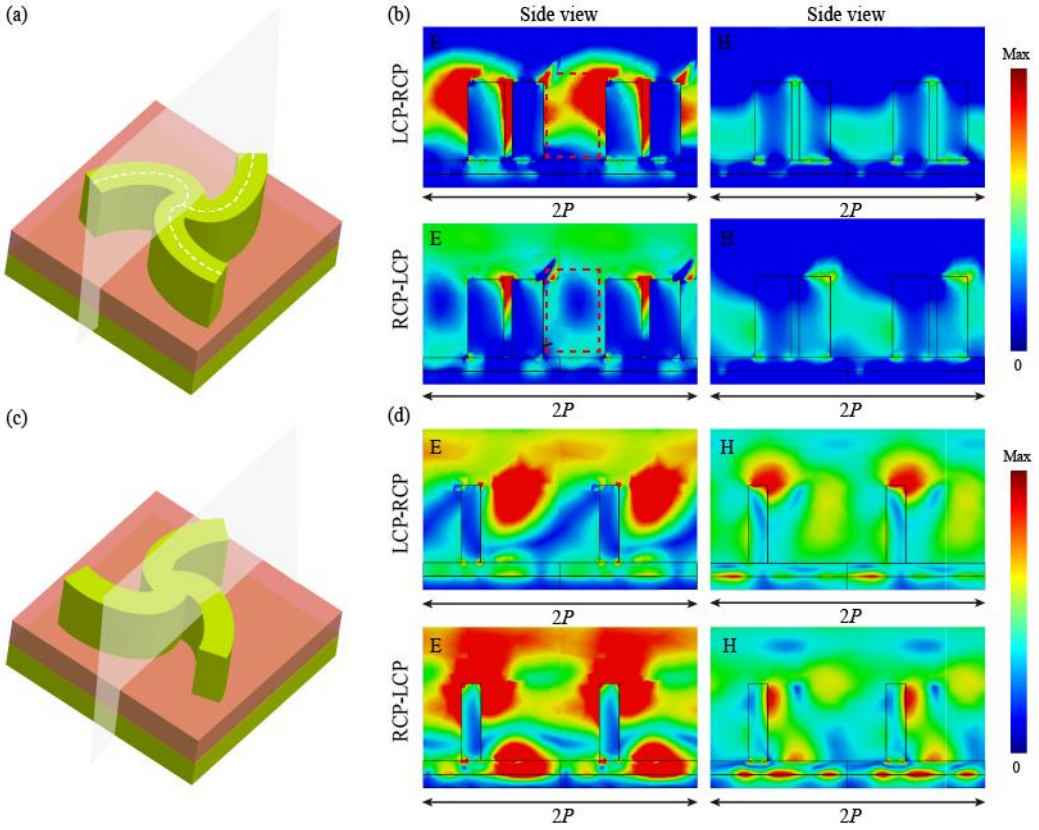



Figure S3 3D views and instantaneous electric and magnetic field distributions. **(a)**, **(c)** 3D views of LS and ALS elements. **(b)**, **(d)** The contour images of instantaneous electric and magnetic field distributions inside view for LCP and RCP illumination at 577 nm.

## S5. Data explanation

The plotted data originates from the theoretical (Matalab) and simulated (CST Microwave Studio) calculations of the software. To achieve broadband spin-selective wavefront manipulation with the generalized PB phase, we design the LS and ALS structure in Figure 1, which demonstrates the generation of the generalized PB phase in a broadband wavelength range. Figure 2 illustrates the instantaneous electric and magnetic field distributions to reveal the physical mechanism of spin-selective wavefront manipulations of LS and ALS structures (data originates from software screenshots). Figure 3 is used to verify the asymmetric and broadband characteristics of the designed scheme, and Figure 4 further demonstrates spin-selective functionality utilizing a bifocal metalens based on the generalized PB phase.